International Journal for Parasitology 52 (2022) 35–45

Contents lists available at ScienceDirect

International Journal for Parasitology

journal homepage: www.elsevier.com/locate/ijpara

Proteomic identification of the contents of small extracellular vesicles from in vivo *Plasmodium yoelii* infection

Karina P. De Sousa [a,1], Jeremy Potriquet [b], Jason Mulvenna [a], Javier Sotillo [b,c], Penny L. Groves [a,2], Alex Loukas [a], Simon H. Apte [b,2], Denise L. Doolan [a,b,*]

[a] Infectious Diseases Programme, QIMR Berghofer Medical Research Institute, Brisbane, QLD 4006, Australia
[b] Centre for Molecular Therapeutics, Australian Institute of Tropical Health and Medicine, James Cook University, Cairns QLD 4878 Australia
[c] Parasitology Reference and Research Laboratory, Centro Nacional de Microbiología, Instituto de Salud Carlos III, Majadahonda, Madrid, Spain

ARTICLE INFO

Article history:
Received 15 March 2021
Received in revised form 7 June 2021
Accepted 14 June 2021
Available online 30 July 2021

Keywords:
Extracellular vesicles
Exosomes
Plasmodium
Malaria
Immunomodulation
Proteomics

ABSTRACT

Small extracellular vesicles, including exosomes, are formed by the endocytic pathway and contain genetic and protein material which reflect the contents of their cells of origin. These contents have a role in vesicle-mediated information transfer, as well as physiological and pathological functions. Thus, these vesicles are of great interest as therapeutic targets, or as vehicles for immunomodulatory control. In *Plasmodium* spp. infections, vesicles derived from the parasite or parasite-infected cells have been shown to induce the expression of pro-inflammatory elements, which have been correlated with manifestations of clinical disease. Herein, we characterised the protein cargo of naturally occurring sEVs in the plasma of *P. yoelii*-infected mice. After in vivo infections, extracellular vesicles in the size range of exosomes were collected by sequential centrifugation/ultracentrifugation followed by isopycnic gradient separation. Analysis of the vesicles was performed by transmission electron microscopy, dynamic light scattering, SDS–PAGE and flow cytometry. LC-MS analysis followed by bioinformatics analysis predicted parasite protein cargo associated with exosomes. Within these small extracellular vesicles, we identified proteins of interest as vaccine candidates, uncharacterized proteins which may be targets of T cell immunoreactivity, and proteins involved in metabolic processes, regulation, homeostasis and immunity. Importantly, the small extracellular vesicles studied in our work were obtained from in vivo infection rather than from the supernatant of in vitro cultures. These findings add to the growing interest in parasite small extracellular vesicles, further our understanding of the interactions between host and parasite, and identify novel proteins which may represent potential targets for vaccination against malaria.

1. Introduction

Extracellular (secreted) vesicles can be divided into three main categories, according to their origin and composition: microvesicles, apoptotic bodies, and exosomes (Raposo and Stoorvogel, 2013). Extracellular vesicles (EVs) below 160 nm in diameter (typically ranging between 40 and 120 nm), originating within the cellular multivesicular endosomal compartments and secreted to the extracellular milieu via an energy-dependent mechanism, are designated as exosomes (reviewed in Mathieu et al., 2019); they represent true subcellular compartments and cannot be defined as mere plasma membrane fragments (Yáñez-Mó et al., 2015). Despite these unique characteristics, the rigorous definition of exosomes is often debated and remains a challenge, as no specific markers exist. To this end, the International Society for Extracellular Vesicles (ISEV) has published guidelines that encourage the use of the term "EV" for secreted lipid bilayer-delimited particles (Théry et al., 2018). Identification of the vesicles as exosomes relies on components that are commonly enriched in these vesicles, such as CD9, CD63 and CD81 (tetraspanins), CD13 and CD26 (surface peptidases), CD55 and CD59 (GPI-anchored molecules), HSP70, ICAM1 and GAPDH (Chaput and Théry, 2011; Lötvall et al., 2014; Keerthikumar et al., 2016; Kowal et al., 2016; Jeppesen et al., 2019). These molecules can be used to identify the vesicles as exosomes, together with transmission electron microscopy (TEM) (Lötvall et al., 2014; Peterson et al., 2015), which remains the gold standard for exosome identification. More recently, different meth-

* Corresponding author at: Australian Institute of Tropical Health and Medicine, James Cook University, Cairns QLD 4878 Australia; Tel.: 61-7-4232 1492.
E-mail address: denise.doolan@jcu.edu.au (D.L. Doolan).
[1] Present address: School of Life and Medical Sciences, Biosciences Research Group, University of Hertfordshire, Hatfield AL10 9AB, UK.
[2] Present address: Queensland Lung Transplant Service Laboratory, Prince Charles Hospital, Brisbane, QLD 4032 Australia.

https://doi.org/10.1016/j.ijpara.2021.06.001
0020-7519/

ods for visualisation and analysis of the vesicles have emerged, such as the Nanoparticle Tracking Analysis (NTA) and Dynamic Light Scattering (DLS), allowing for more comprehensive identification and characterisation of these nanovesicles.

Historically, exosomes have been shown to contain different types of lipids and nucleic acids (Valadi et al., 2007; Mathieu et al., 2019) as well as multiple active enzymes (Yáñez-Mó et al., 2015). In the case of infectious diseases, exosomes have been implicated in the pathogenesis of HIV (Gould et al., 2003; Nguyen et al., 2003), Kuru and Creutzfeld-Jakob disease (Fevrier et al., 2004), toxoplasmosis (Bhatnagar et al., 2007), leishmaniasis (Silverman and Reiner, 2012), trypanosomiasis (Geiger et al., 2010; Bayer-Santos et al., 2013) and malaria (Regev-Rudzki et al., 2013), among others, serving also as immunomodulators in all known pathogen classes (reviewed in (Schorey et al., 2015)).

In malaria, there is evidence of vesicle-mediated information transfer between infected cells, including trafficking of drug resistance markers under conditions of drug selection (Regev-Rudzki et al., 2013) and factors that promote differentiation to sexual forms (Mantel et al., 2013; Regev-Rudzki et al., 2013). Furthermore, EVs have been associated with the most severe manifestation of the disease, cerebral malaria (Combes et al., 2004; Nantakomol et al., 2011; Mantel et al., 2013), potentially as a consequence of the excessive activation of immune cells releasing pro-inflammatory cytokines and other immunomodulatory effects (Clark and Rockett, 1994; Sisquella et al., 2017; Sampaio et al., 2018).

Due to the inherent properties of exosomes, namely biological relevance, biocompatibility, ease of cellular uptake and wide-ranging roles, the interest in these vesicles as tools for immune mediation, namely as vaccine candidates, has been dramatically increasing. In line with this, it has been shown that exosomes and/or exosome-derived antigens promote T and B cell immunity (Bhatnagar et al., 2007; Giri et al., 2008; Martin-Jaular et al., 2011; Gutzeit et al., 2014; Montaner-Tarbes et al., 2016). T cells can be activated by the direct presentation of major histocompatibility complex (MHC) –peptide complexes on the exosome surface to antigen-specific T cells, or by cross-presentation of antigens carried by exosomes after internalisation and additional processing of these antigens (Thery et al., 2002; Montecalvo et al., 2008; Robbins and Morelli, 2014; Shenoda and Ajit, 2016).

The pioneering work from Martin-Jaular et al. (2011) showed that mice immunised with exosomes purified from *Plasmodium yoelii* could induce production of IgG antibodies capable of recognising infected cells and confer long-lasting protection against lethal challenge with the parasite, and performed LC–MS/MS based proteomics to demonstrate the presence of *P. yoelii* proteins in isolated exosomes from plasma of infected mice. More recently, work from the same group (Martin-Jaular et al., 2016) showed that EVs isolated from the plasma of *Plasmodium vivax*-infected donors were actively taken up by human splenocytes, resulting in changes in T cell subsets, and that these EVs facilitate the adherence of non-circulating parasites, contributing to the evasion mechanisms of *Plasmodium* (Toda et al., 2020). Studies were also performed by others to test small EV (sEV)-based transmission-blocking vaccines that target the sexual stage of the *Plasmodium* parasite as anti-malarial vaccines (Dinglasan et al., 2013), albeit with limited results. As such, there is a need to further our knowledge on the immunomodulatory molecules that are contained within extracellular vesicles, including exosomes, deriving from *Plasmodium* or *Plasmodium*-infected cells, as targets for protective immunity against malaria.

2. Materials and methods

A schematic of the experimental methods used herein to identify and characterise proteins within naturally occurring sEVs from *P. yoelii* infections is provided in Fig. 1. Two independent experiments of the complete comprehensive pipeline were conducted.

2.1. Establishment of the P. yoelii 17XNL strain rodent blood stage malaria infection

Following an established method of infection with *Plasmodium* spp. parasites, $1x10^5$ cryopreserved *P. yoelii* 17XNL-infected parasitized red blood cells (pRBC) were delivered intraperitoneally to two specific pathogen-free female C57BL/6 mice (Animal Resource Centre, Australia) at 6–9 weeks of age, for establishment of a pre-infection. Seven days post-infection (days p.i.), blood was drawn from the distal end of the caudal vein. The percentage of parasitized red blood cells was determined by microscopic assessment of thin blood smears stained using the Diff-Quick staining system (MilliporeSigma, USA). From the animal with the highest parasitaemia (23% at 18 days p.i), blood was collected from the distal end of the caudal vein into sterile PBS. Female C57BL/6 mice (n = 40) mice were infected with 1×10^5 *P. yoelii* 17XNL parasites via the caudal vein. Naïve, uninfected mice were used as controls (n = 40).

2.2. Determination of mouse parasitaemia

The flow cytometric assessment of blood (FCAB) assay was used to determine peripheral blood parasitaemia of infected mice, at each time point (Apte et al., 2011). Briefly, an aliquot of the blood collected by cardiac puncture was diluted in Macs Buffer (MB, 0.2 mM EDTA, 0.5% FCS in 1× PBS), and the suspension was transferred into wells of a 96-well V-bottom plate and centrifuged at 4 °C and 600*g* for 4 min. Supernatant was discarded and cells were lysed and fixed with sterile-filtered PBS with 4% w/v paraformaldehyde and 0.0067% w/v saponin for 10 min at 37°C. Cells were washed and resuspended in dye solution, consisting of 1:1000 Hoescht 3342 dye in Macs buffer (MB), and samples were run on an high throughput system (HTS)-equipped BD LSR II Fortessa™ flow cytometer (BD Biosciences, USA).

2.3. Isolation and purification of sEVs from plasma

Peripheral blood was collected from C57BL/6 mice pre-infection or at 7, 8 or 9 days p.i. with *P. yoelii* 17XNL pRBCs (n = 10 mice/-timepoint). The plasma was separated by centrifugation of whole blood at 2000*g* for 15 min, and stored at −20°C until further use. Plasma was pooled per timepoint, diluted 1:1 with PBS, and centrifuged for 30 min at 2000*g* (AllegraX-14R, Beckman Coulter, Australia). The supernatant was transferred to new tubes and centrifuged for 45 min at 15,000*g*. Resulting supernatant was collected and centrifuged at 100,000*g* for a further 2 h. The pellet was resuspended in PBS, filtered through a 0.2 µm syringe filter (Acrodisc® Syringe Filters, Pall Corporation, Australia), and centrifuged for a further 2 h at 100,000*g*. All centrifugation steps were performed at 4°C in order to maintain vesicle stability. The final pellet was resuspended in Dulbecco's PBS (dPBS). Isopycnic separation was used to further purify sEVs using sequential ultracentrifugations in an OptiPrep™ (Sigma-Aldrich, USA) iodixanol gradient, as follows. Vesicle suspensions obtained from the differential centrifugations were subjected to a 0.25 M sucrose and iodixanol density gradient (5–40%). Gradients were prepared in Polyallomer 14 × 89 mm thin-wall tubes (Beckman Coulter, USA), under sterile conditions. A volume of 200 µL vesicle suspension was added to each gradient column and centrifuged for 18 h, at 4 °C and 100,000*g*. After centrifugation, 12 × 1 mL fractions representing fractions corresponding to an iodixanol density of approximately 1.15 g/mL (density typically associated with exosomes), numbered 1 to 12 for each infected and control group were collected at 0, 7, 8

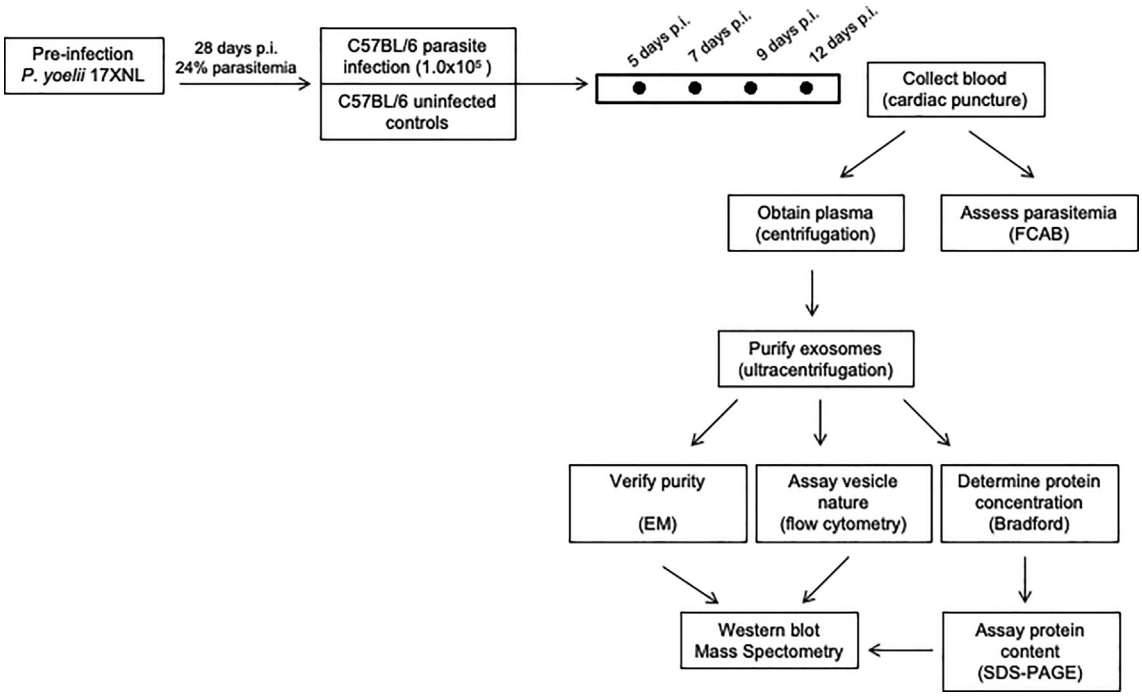

Fig. 1. Flow chart for the analysis of proteins contained within extracellular vesicles following in vivo *Plasmodium yoelii* infection. C57BL/6 mice (n = 10/group) were infected with 1×10^5 *P. yoelii* parasitized red blood cells. Blood was collected by cardiac puncture at days 0, 7, 8 and 9 p.i. for assessment of parasitaemia and isolation of exosomes. Exosomes were purified by ultracentrifugation (30 min at 2000*g*; 45 min at 15,000*g*; 100,000*g* for 2 h followed by filtration through a 0.2 μm syringe filter) and isopycnic separation (5–40% iodixanol density gradient in 0.25 M sucrose). The identity of the purified vesicle was confirmed by dynamic light scattering, SDS-PAGE, flow cytometry and transmission electron microscopy (EM). Protein concentration was determined by Bradford assay. Exosome samples were lysed to release the internal proteins which were chemically processed for analysis by tandem mass spectrometry. Full scan Time-of-Flight mass spectrometry (IDA) data was acquired over the mass range of 300–2000 (m/z) with 250 ms accumulation time and, for product ions, 100–2000 (m/z) with 100 ms accumulation time for a total of 4152 cycles. Samples from age-and sex-matched infected and uninfected mice were passed simultaneously through MS to avoid false-positives. Resulting spectra were queried against relevant databases: National Center for Biotechnology Information (NCBI) (https://www.ncbi.nlm.nih.gov/), European Bioinformatics Institute (EMBL-EBI) (http://www.ebi.ac.uk), UniProt (http://www.uniprot.org), Gene Ontology (GO) (http://geneontology.org), Panther Classification System (http://pantherdb.org), Ensembl (http://www.ensembl.org/index.html), PlasmoDB v39 (http://plasmodb.org/plasmo) and ExoCarta v5 (http://exocarta.org/index.html) to identify the proteins and their putative annotation. Blood collected from age-and sex-matched uninfected C57BL/6 mice was processed in parallel as a negative control. days p.i., days post-infection; EM, electron microscopy.

and 9 days p.i. from each gradient column. To avoid contamination with iodixanol on downstream processing and analysis, gradient-purified sEVs were further subjected to three rounds of washing with dPBS, by centrifugation for 1 h at 100,000*g*, at 4°C. Samples were stored at −80°C until further use

2.4. Dynamic Light Scattering (DLS) analysis

Control and infected samples were diluted 1:10 in PBS to ensure an optimum of 50–200 kilocounts per second. DLS analysis was performed on a Zetasizer Nano ZP3600 (Malvern Instruments Ltd., UK). All measurements were made in triplicate, using independent aliquots.

2.5. Transmission electron microscopy (TEM)

An aliquot from each of the samples prepared in Tris-HCl solution (pH 7.5) was directly adsorbed onto glow-discharged formvar-carbon coated copper grids on SuperFrost slides (AgarScientific, UK), which were next negatively stained with freshly prepared 2% uranyl acetate (SigmaAldrich) in aqueous suspension and air-dried for 3 min. Digital images were taken with a JEM-100CX transmission electron microscope (JEOL, Japan) equipped with an Olympus Morada camera (Olympus, Japan), up to 200,000× magnification and using exposure times between 100 and 400 ms.

2.6. Multiparametric flow cytometry

Pooled samples from control and infected groups (50 μL) were added to diluted monodisperse polystyrene 1 μm anti-mouse reference beads (Sigma-Aldrich) and incubated for 15 min at room temperature (RT). Samples were further diluted with 500 μL of MB and incubated overnight at 4°C under continuous slow rotation, in order to adsorb the exosomes to the beads. Next, samples were incubated with 500 μL of 100 mM glycine (SigmaAldrich) for 30 min at RT, then washed and stained with a pool of surface marker antibodies (FITC-antiCD9, PerCP/Cy5.5-antiCD63, AF647-antiCD55 and PE-antiCD59) (BioLegend, USA) at 4°C for 1 h, and then washed again to remove unbound stain. Vesicles were resuspended in MB prior to data acquisition using a BD LSR II Fortessa™ flow cytometer and analysed with FlowJo software vX.0.6 (FlowJo LLC, USA).

2.7. SDs-PAGE

SDS-PAGE protein profiles of the isolated sEVs were obtained using a standard Bis-Tris system and a XCell SureLock Mini-cell electrophoresis system (Bio-Rad, USA). Ten μL of 4× Laemmli Sample Buffer (SigmaAldrich) were added to each of the samples and incubated for 5 min at 95 °C prior to electrophoretic separation on a 12% acrylamide gel under a constant voltage of 90 V in Bis-Tris buffer. Gels were washed with water and stained with Coomassie Brilliant Blue SigmaAldrich) for 3 h at RT with constant agitation. Unbound stain was removed by submersion of gels in a

solution of 10% methanol:5% glacial acetic acid until blue bands were visible on a clear background. Molecular weight standards were used for assessment of protein mass.

2.8. Filter-aided sample preparation (FASP) purification and protein alkylation

Density gradient fractions indicated by electron microscopy to contain sEVs were subjected to three rounds of high-speed centrifugation for 1 h at 100,000*g* at 4°C. The resultant pellet was resuspended in 1% SDS in PBS, and 50 mM tetraethylammonium bromide (TEAB; SigmaAldrich) added. Samples were vortexed and incubated for 15 min at RT with constant slow agitation. Proteins were purified using a modified FASP protocol (Wiśniewski et al., 2009). Briefly, total proteins from lysed exosome preparations were reduced with 20 mM dithiothreitol (DTT, SigmaAldrich) for 5 min at 95°C, and then alkylated with 40 mM iodoacetamide (IAA, SigmaAldrich) for 45 min at RT in the dark. Samples were next diluted by eight volumes of 8 M Urea, 10% isopropanol in 100 mM TEAB, transferred into a 30 kDa cut-off Acroprep advance 96 filter plate (PALL) and centrifuged at 3000*g* for 30 min. This was followed by four consecutive wash and centrifugation steps (3000*g*, 40 min) where the first two washes were performed with 8 M Urea,10% isopropanol in 100 mM TEAB and the final two with 100 mM TEAB. Trypsin (SigmaAldrich) was then added to a final ratio of 1:50 trypsin:protein and samples were incubated overnight at 37°C. The samples were then centrifuged at 3000*g* for 20 min, and 50 mM TEAB added to recover left-over peptides. The flow-through was collected and dried in a speed-vacuum (Savant SVC-100H Speedvac Concentrator, ThermoFisher Scientific, Australia) before re-solubilization in 0.1% trifluoroacetic acid (TFA; SigmaAldrich) aqueous solution.

2.9. Tandem mass spectrometry

To facilitate mass spectral analysis, tryptic peptides were desalted on a ZipTip C_{18} pipette tip (Millipore). Briefly, C_{18} tips were washed five times with 10 µl of 70% acetonitrile (ACN; SigmaAldrich)/0.1% TFA, then equilibrated with a 0.1% TFA solution. Peptides were loaded onto the tips by pipetting and bound peptides were washed five times with a solution of 0.1% TFA, and eluted in 70 µl of 70% ACN/0.1% TFA. Desalted peptides were lyophilized (Savant SVC-100H Speedvac Concentrator; ThermoFisher Scientific, Australia) at 37 °C, resuspended in 0.1% formic acid [aq]/2% ACN, centrifuged at 12,000*g* for 1 min and fractionated using reverse-phase chromatography. Peptides were desalted for 10 min using 0.1% formic acid [aq]/5% acetonitrile in an Eksigent cHiPLC column (Eskigent Technologies; USA) which was then placed in-line with an analytical cHiPLC column (Eskigent Technologies). Full-scan Time-of-Flight mass spectrometry (TOF-MS) data was acquired in an Information Dependant Acquisition (IDA) mode on a triple-TOF 5600 (AB Sciex, USA) over the mass range 300–2000 (m/z) with 250 ms accumulation time and, for product ions, 100–2000 (m/z) with 100 ms accumulation time for a total of 4152 cycles. Ions observed in the TOF-MS scan, exceeding a threshold of 50 counts and possessing a charge state of +2 to +4, were set to trigger the acquisition of product ion spectra for a maximum of 10 of the most intense ions. Dynamic exclusion was incorporated for 10 s after two occurrences of a precursor ion. A scan of the reference compound (Glufibrinopeptide B) was acquired every 10 scans of the analyte through the entire run. Data was acquired and processed using Analyst TF1.5.1 software (AB Sciex Pte. Ltd, USA). Samples from age-and sex-matched uninfected mice were passed through MS simultaneously with samples from infected mice as a negative control.

2.10. Spectral searches and protein annotation and categorization

Spectral searches of LC–MS/MS data were conducted on Protein Pilot (AB Sciex) with the following parameters: one miss cleavage permitted, carboxymethylation specified as a fixed modification and oxidation of methione as a variable modification, background correction used, and biological modifications specified as an ID focus. Results were validated using MASCOT Daemon v2.5 (Matrix Science, USA). Searches were conducted against general protein databases, parasite-specific and exosome-specific databases using standard parameters, as follows: for general annotation, including mouse-specific annotation, the following databases were prospected: National Center for Biotechnology Information (NCBI) (https://www.ncbi.nlm.nih.gov/), European Bioinformatics Institute (EMBL-EBI) (http://www.ebi.ac.uk), UniProt (http://www.uniprot.org), Gene Ontology (GO) (http://geneontology.org), Panther Classification System (http://pantherdb.org) and Ensembl (http://www.ensembl.org/index.html). For parasite-specific annotation, the PlasmoDB v39 (http://plasmodb.org/plasmo) database was used. For exosome-specific annotation, ExoCarta v5 (http://exocarta.org/index.html) was prospected. The mass spectrometry proteomics data have been deposited to the ProteomeXchange Consortium via the PRIDE partner repository with the dataset identifier PXD011285.

2.11. Statistical significance

Data were analysed using Prism software v6.05 (GraphPad, USA). Statistical significance was determined using two-tailed Student's *T* test, unless otherwise stated, with $P < 0.05$ considered as significant.

3. Results

Infection with *Plasmodium* is associated with increased levels of circulating microparticles, including exosomes (Couper et al., 2010; Deolindo et al., 2013; Mantel et al., 2013; Regev-Rudzki et al., 2013; Mantel and Marti, 2014), and studies in several disease models have shown that exosomes and other sEVs contain proteins that can play a role in immune modulation (Schorey et al., 2015). Some studies have provided preliminary information on vesicle-associated factors involved with this immunopathological process (Mantel et al., 2013; Mantel and Marti, 2014; Sisquella et al., 2017; Babatunde et al., 2018; Demarta-Gatsi et al., 2019; Toda et al., 2020). However, the exact identity of the primary *Plasmodium* products that promote the dysregulation of the immune and haematological systems upon infection is still largely unknown, as are the potentially important immunoreactive targets of host/-parasite interactions. It is possible that vesicles released from the parasite or host infected cells can facilitate the transfer of such factors and products, as well as promote cellular effector functions (Rechavi et al., 2009; Mittelbrunn and Sánchez-Madrid, 2012).

3.1. sEVs isolated from the plasma of P. yoelii –infected mice are of exosomal nature

Guidelines for the identification of exosomes and other vesicles, established in 2018 by ISEV (Théry et al., 2018), recommend the use of at least two different approaches when analysing extracellular vesicles, as well as visualisation by TEM. In accordance with those guidelines, herein vesicles were isolated by ultracentrifugation and further purified by isopycnic separation and then analysed by DLS, flow cytometry and TEM.

All DLS measurements were performed on independent triplicates from aliquots of the isolated vesicles. Results showed that

the vesicles from all groups were homogeneous in size (median diameter of 142.2 ± 11 nm) (Table 1, Supplementary Fig. S1), consistent with the expected value. DLS also provided data on the polydispersity index (PDI), zeta-potential (zP), electrophoretic mobility and conductivity of the samples (Table 1). The vesicles were shown to have a PDI ranging from 0.3 to 0.7, indicating adequate size dispersion for measurement with this technique (Instruments, 2009).

The zP of the vesicles purified from the plasma of infected and control mice was negative in all cases, varying between −7.36 and −0.86 mV (Table 1), indicating a weak negative charge. Electrophoretic mobility values for these samples varied between −0.4 and −0.7, corroborating results obtained for zP. Conductivity values for the samples ranged from 10 to 15 mS/cm (Table 1), consistent with a relatively high saline concentration, as expected since the samples were diluted in PBS.

The isolated vesicles were also analysed by TEM. Isopycnic purification resulted, as described, in 12 fractions of different densities for each time point (0, 7, 8 and 9 days p.i.) for a total of 48 fractions. All these fractions were analysed by TEM, revealing that only one fraction per time point (for both control and infected mice) was positive for vesicles, consistent with a pure preparation. The positive fraction corresponded to an iodixanol density of ~1.15 g /mL, matching data reported in the literature (Vlassov et al., 2012; Padro et al., 2013; Kowal et al., 2016). TEM analysis also revealed a relatively homogeneous population of vesicles under 150 nm in diameter (Fig. 2). These results were consistent with published literature regarding exosome size, structure and shape (Conde-Vancells et al., 2008; Couper et al., 2010; Martin-Jaular et al., 2011; Hosseini-Beheshti et al., 2012).

Additional characterization of the isolated vesicles used flow cytometry to identify surface molecules commonly reported for exosomes (Clayton et al., 2003; Keerthikumar et al., 2016). Accordingly, vesicles were adsorbed onto 1 μm aldehyde/sulfate latex beads by passive adsorption, washed and stained with anti -CD9, -CD63, -CD55 and -CD59 antibodies conjugated with fluorescent markers, and visualised by flow cytometry. The presence of these molecules in the analysed fractions added confidence to the identification of the isolated sEVs as exosomes (Supplementary Fig. S2).

sEV preparations isolated from infected and uninfected mice (pooled for each group) were compared by electrophoretic separation on an SDS-PAGE gel followed by Coomassie staining (Supplementary Fig. S3), showing distinct proteomic profiles for infected versus uninfected mice. Additionally, no bands were visible at ~20 kDa, indicating that the preparation was free from contaminating haemoglobin (Mantel et al., 2013).

3.2. Changes in Plasmodium-infected blood correlate with increasing parasitaemia and sEV levels

Plasmodium yoelii-infected mice produced a standard blood-stage parasitaemia curve peaking at 9 days p.i. with a mean of 16.3% (range: 5.1–29.6% pRBC) (Fig. 3) as determined by FCAB assay (Apte et al., 2011). To determine if the *P. yoelii* infection was associated with an increase in protein content which could be associated with the secretion of sEVs, infected and control samples were analysed for particle numbers (peak intensity) using DLS, and total protein concentration using the Bradford protein assay. Results showed that mice infected with *P. yoelii* had a higher number of circulating sEVs compared with uninfected controls and this peaked at 9 days p.i. (fold increase of 2.65; peak intensity of 82% for infected mice versus 30.9% for uninfected mice) with a 5.4-fold increase in total protein concentration (0.3 mg/mL on day 0, 63 mg/mL on day 9) (Fig. 4). A significant positive correlation between parasitaemia and total protein concentration was apparent (Fig. 5), consistent with an increase in protein cargo or parasite- and/or host-derived sEVs (and efficient protein trafficking into exosomes and exosome-like vesicles).

3.3. Circulating sEVs contain host-derived and parasite-derived proteins

Next, the protein cargo of the sEVs was evaluated. For that purpose, the preparations were further purified by isopycnic separation followed by three rounds of ultracentrifugation, and subjected to FASP, followed by tryptic digestion and liquid chromatography-tandem mass spectrometry (LC–MS/MS). Peptides resulting from the LC–MS/MS were identified using the software Protein Pilot (AB Sciex Pte. Ltd) against several relevant human-, parasite- and exosome- specific databases, as detailed in Section 2.10. Identified hits included proteins that confirmed the exosomal nature of the sEVs found in our preparations, since they are often found in exosomes and classified in the top 25 exosomal protein markers in ExoCarta, namely CD9, CD63, HSP8, GAPDH, ANXA2, YWHAZ, ALB, EEF1A1 and ALDO (Supplementary Table S1). Notably, integrins and tetraspanins, which are also considered important exosomes indicators, were also identified (Andreu and Yanez-Mo, 2014; Willms et al., 2018). Markers of other vesicles such as microvesicles (CD40L), membrane vesicle markers (CD133) or apoptotic vesicles (histones) could not be found in the preparations, confirming the purity of the samples. In total, 383 unique proteins were identified originating from the host, after excluding repeats (Supplementary Table S2) (complete list of proteins is available on the ProteomeXchange Consortium website via the dataset identifier PXD011285).

3.4. Classification of host-derived proteins identified in sEVs

Of the 489 proteins identified from samples obtained on 7, 8 and 9 days p.i. using LC–MS/MS (ProteomeXchange Consortium dataset PXD011285), 360 proteins were host-associated proteins, of which 38 proteins were found only in control uninfected mice, 177 proteins were found only in infected mice, and 145 proteins were found in both infected and uninfected mice (Fig. 6). Using the Gene Ontology Resource, host-derived proteins identified within sEVs by LC/MS-MS were implicated with biological processes, molecular function, transport and regulatory activity, as well as immune responses (Supplementary Fig. S4). This list included integrins (Itga2, Itgb1, Itgb3) as well as several proteins associated with host immunity, including CD71 (Table 2). Overall, 43% of all proteins were associated with activity on lipid and nucleic acid binding, while 12% were associated with the cytoskeleton (annexin, actin, keratin, moesin and others), macrophage activation and glycolysis. Our data are consistent with reports of a role for these vesicles in the immune system response (Hwang, 2013; Robbins and Morelli, 2014), and with reports by others identifying *P. yoelii* proteins within exosomes during an infection (Martin-Jaular et al., 2011; Martín-Jaular et al., 2016).

Using the data obtained from the LC/MS-MS analysis, the identified proteins were also classified by time points (7, 8 and 9 days p.i.) and gene ontology. This analysis provided information about the dynamics of protein expression in this *P. yoelii* rodent model and the influence of *Plasmodium* infection on the protein cargo (Supplementary Fig. S5).

3.5. Circulating sEVs contain parasite-derived proteins that are potential targets for protective immunity

Overall, 129 proteins associated with the parasite were found in the sEV preparations (complete list of proteins is available on the ProteomeXchange Consortium website via the dataset identifier PXD011285). The majority of these proteins have not been previ-

Table 1
Dynamic Light Scattering results of samples containing extracellular vesicles isolated from *Plasmodium yoelii*-infected mice.

Days p.i.	Sample ID	Size (nm)	PDI	zP (mV)	Electrophoretic Mobility (μmcm/Vs)	Conductivity (mS/cm)
7	7-Control	141.3	0.706	−7.23	−0.5694	10.7
	7-Infected	145.1	0.685	−6.38	−0.5024	14.4
8	8-Control	136.7	0.709	−7.08	−0.5907	14.3
	8-Infected	162.2	0.309	−5.50	−0.4333	15.7
9	9-Control	129.4	0.709	−7.36	−0.6958	11.9
	9-Infected	138.7	0.684	−0.86	−0.6780	10.6

PDI, polydispersity index; zP, zeta potential.

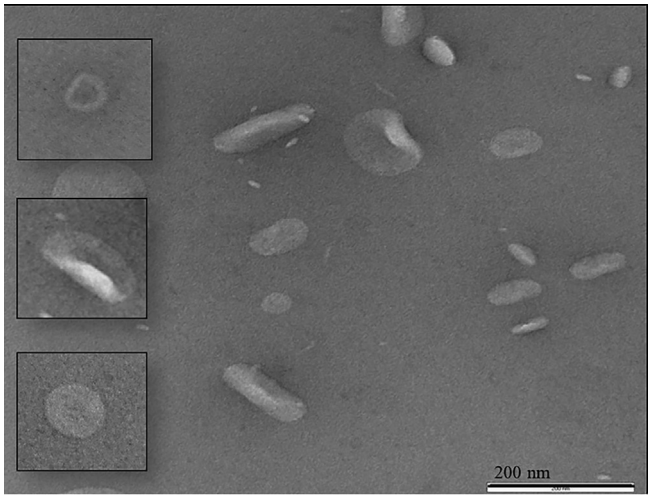

Fig. 2. Representative Transmission Electron Microscopy photos of nanovesicles isolated from the plasma of C57BL/6 mice infected with *Plasmodium yoelii* 17XNL. Images presented here show negatively-stained exosomes, imaged by TEM at an amplification of 150 K. Insets are representative of single vesicles in other photos of the same fraction. Bar represents 200 nm.

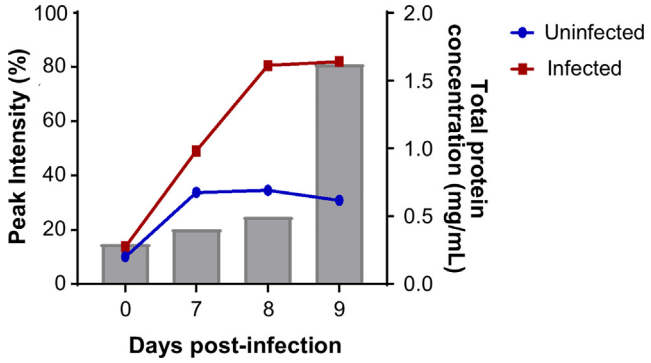

Fig. 4. Levels of secreted vesicles and total protein concentration of small extracellular vesicles isolated from *Plasmodium yoelii* 17XNL–infected C57BL/6 mice. Vesicles isolated by ultracentrifugation followed by isopycnic separation were subject to Dynamic Light Scattering analysis to measure the number of secreted vesicles. DLS analysis was performed at an optimum of 50–200 kilocounts per second using a 633 nm He-Ne laser operated at a fixed angle of 173° at a controlled temperature of 25 °C. The Bradford protein assay was used to measure total protein concentration of lysed vesicles (λ = 595 nm). Vesicle number represented on the left Y axis (peak intensity in %); total protein concentration of lysed vesicles represented on the right Y axis (concentration in mg/mL). Grey histograms represent peak intensity. Red and blue lines represent the total protein concentration for infected or uninfected mice, respectively.

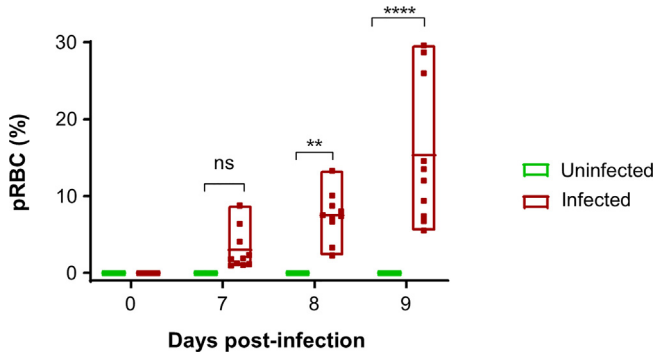

Fig. 3. Blood-stage parasitaemia of *Plasmodium yoelii*-infected mice. C57BL/6 Mice (n = 10/group per timepoint) were infected with 1×10^5 *P. yoelii* 17XNL parasitized red blood cells and assessed for parasitaemia pre-infection (0 days p.i.) or days 0, 7, 8 or 9p.i. by the flow cytometric assessment of blood assay. Dunnett's multiple comparison test was used to assess the statistical significance of the increase in parasitaemia during infection; ns, not significant (P > 0.005); **P = 0.005; ****P = 0.001.

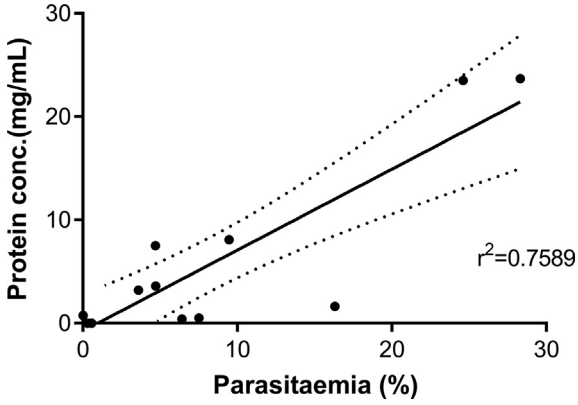

Fig. 5. Correlation between parasitaemia and the concentration of extracellular vesicle-derived proteins from *Plasmodium yoelii*-infected mice. Pearson correlation coefficient was determined from 12 matched pairs (representing parasitaemia and corresponding total protein concentration) with a 95% confidence interval. The dotted lines represent the confidence interval. The linear correlation was determined as significantly deviant from zero (P = 0.0001; r^2 = 0.76).

ously characterised. After controlling for the number of unique peptides identified (cut-off set at #hits ≥ 2), 40 proteins could be confidently reported (Table 3). Importantly, this list included proteins of interest as vaccine targets, such as the p235 rhoptry protein, multiple members of the *yir* multi-gene protein family, the Asparagine-rich protein, and the ribosomal protein S12.

Although the majority of the parasite proteins identified in circulating sEVs derived from *P. yoelii* are still uncharacterized, their predicted biological functions based on sequence similarity and functional domain comparative analysis indicated roles associated with parasite biology and metabolism. Analysis of the stage specificity of these potential vaccine targets could not be performed due to the lack of known transcriptomic data (www.PlasmoDB.org). However, analysis of compartment specificity of the uncharacterized proteins was performed using PANTHER (Mi et al., 2013), revealing that some of those proteins were localised to the apical complex and suggestive of a possible role in invasion processes.

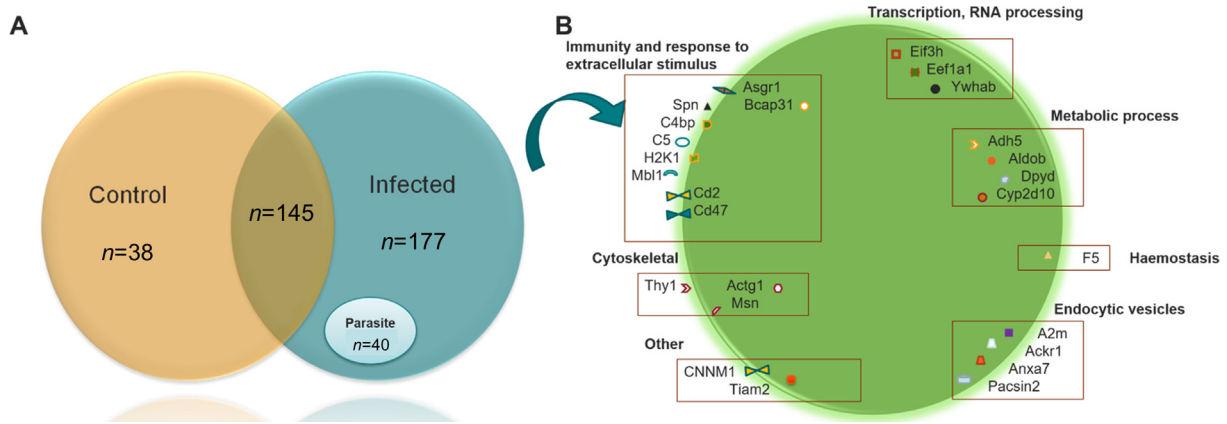

Fig. 6. Proteins identified within small extracellular vesicles isolated from *Plasmodium yoelii* 17XNL–infected C57BL/6 mice. (A) From a total of 489proteins identified from samples obtained on days 7, 8 and 9p.i., 360 proteins were host-associated proteins, of which 38 proteins were found only in control uninfected mice, 177 proteins were found only in infected mice, and 145 proteins were found in both infected and uninfected mice. (B) Main protein groupings (representative results) for host proteins found within exosomes, reflecting the content of the cells they originated from, are consistent with previous reports and were associated with a range of different molecular classes and functions.

Table 2
Host proteins identified in small extracellular vesicles (sEVs) isolated from *Plasmodium yoelii*-infected mice, associated with host immunity.

UniProt ID	Description/Name	Biological function	Days p.i.
Q6GQT1	Alpha-2-macroglobulin-P	Cytokine, serine protease inhibitor, complement component	8
P34927	Asialoglycoprotein receptor 1	Immunoglobulin receptor superfamily cell adhesion molecule	7
Q61335	B-cell receptor-associated protein 31	MHC class I protein binding, protein complex binding	7
Q9QUI6	Atypical chemokine receptor 1 (CD234)	Duffy antigen/chemokine receptor	8
P08607	C4b-binding protein (C4bp)	Apolipoprotein, receptor metalloprotease, serine protease, complement component, cell adhesion molecule	8
O88783	Coagulation factor V	Apolipoprotein membrane-bound signalling molecule receptor metalloprotease, cell adhesion molecule	8
P06684	Complement C5 (Haemolytic complement)	Cytokine, serine protease inhibitor complement component	8
P01902	H-2 class I histocompatibility antigen	Histocompatibility antigen	8
P55065	Phospholipid transfer protein	transfer/carrier protein, antibacterial response protein	8
Q9CQW9	Interferon-induced transmembrane protein 3 (Dispanin)	Antiviral response protein	7
P11438	Lysosome-associated membrane glycoprotein 1 (LAMP-1)	membrane trafficking regulatory protein	7
Q5DTT8	Paraneoplastic antigen-like protein 5	Defense/immunity protein	8
P39039	Mannose-binding protein A (MBP-A)	Defense/immunity protein	8
E9Q8B5	Complement factor H (Protein Gm4788)	Apolipoprotein, receptor, metalloprotease, serine protease complement component cell adhesion molecule	8
Q8HWB2	Protein H2-Q4	Immunoglobulin receptor superfamily major histocompatibility complex antigen	8
P08920	T-cell surface antigen CD2	membrane-bound signalling molecule, immunoglobulin receptor superfamily, cell adhesion molecule	8
Q9QWK4	CD5 antigen-like (CD5-L)	Receptor, serine protease, oxidase	7, 8, 9
P28665	Murinoglobulin-1	Cytokine, serine protease inhibitor, complement component	7, 8, 9
Q61735	CD47	Immunoglobulin receptor superfamily, guanyl-nucleotide exchange factor, immunoglobulin receptor superfamily, cell adhesion molecule	9
Q6ZPF3	T-lymphoma invasion and metastasis-inducing protein 2 (Tiam-2)	Signalling molecule, guanyl-nucleotide exchange factor	7
Q07797	Galectin-3-binding protein	Transfer/carrier protein, antibacterial response protein	8
P01029	Complement C4 B	Receptor, serine protease, oxidase	8, 9
U6DY13	CD71	Transferrin receptor protein 1	8, 9
P98064	Mannan-binding lectin serine protease 1	Serine protease	8
P14483	H-2 class II histocompatibility antigen	Peptide antigen binding	8

4. Discussion

Exosomes are implicated with numerous biological and pathological processes across many different types of organisms. Beyond serving as a means to convey information in the form of cytokines, genetic material, proteins, peptides and other elements (Yáñez-Mó et al., 2015; Mathieu et al., 2019), these vesicles have an enormous potential in the field of vaccinology against infectious diseases, due to their inherent biological properties (Sampaio et al., 2017; Mekonnen et al., 2018; Drurey et al., 2020).

One of the seminal studies to provide evidence that exosomes derived from *Plasmodium*-infected red blood cells can induce immune responses and protection against lethal infections used the well-established rodent model of malaria, *P. yoelii* 17XNL (Martin-Jaular et al., 2011). We also used this model since it is an in vivo model known to accurately represent infection with other *Plasmodium* spp., including human *Plasmodium* spp. parasites, and in particular *P. vivax* which preferentially infects young reticulocytes. Additionally, in this model, higher parasitaemias can be achieved following controlled infection, thus maximising the num-

Table 3
Parasite-derived proteins identified in small extracellular vesicles (sEVs) isolated from *Plasmodium yoelii* infected mice.

PlasmoDB ID	Description/Name	Biological function (GO)	DPI	Unique peptides (95%)
Characterised proteins (n = 17)				
PY05539	UBA2-related	SUMO activating enzyme activity	8	24
PY00976	Capn7-related	endopeptidase activity	8	11
PY04051[a]	U5 snRNP 100 kD protein	nucleic acid binding	*8*	*8*
PY01185[a]	p235 kDa rhoptry protein	n/a	*8*	*7*
PY02760[a]	bir1 protein	n/a	*8*	*6*
PY01989[a]	Phosphoryn	n/a	*8*	*4*
PY04387[a]	Fimbriae-associated protein 1	n/a	*8*	*4*
PY05570[a]	CPW-WPC domain	n/a	*8*	*4*
PY05324	Ribosomal protein S12	structural constituent of ribosome	8	4
PY03337	Ubiquitin	n/a	8	4
PY00879	CCAAT-box DNA binding protein subunit B	microtubule binding; microtubule motor activity	8	3
PY00078	Dynein beta chain, ciliary	microtubule motor activity	8	3
PY02627	Elongation factor Tu family	translation elongation factor activity	8	3
PY06971[a]	rRNA adenine N(6)-methyltransferase	rRNA-dimethyltransferase activity	*8*	*3*
PY02583	Adaptor complexes medium subunit family	n/a	8	2
PY00810	DNA repair protein RAD54	ATP binding	8	2
PY05730	Neurofilament-H	n/a	8	2
Uncharacterized proteins (n = 23)				
PY02829	Uncharacterized protein	n/a	8	104
PY04477	Uncharacterized protein	Sigma factor activity	8	13
PY06181	Uncharacterized protein	n/a	8	9
PY04486	Uncharacterized protein	n/a	8	6
PY07433	Uncharacterized protein	n/a	8	6
PY01436	Uncharacterized protein	n/a	8	5
PY04880	Uncharacterized protein	n/a	8	4
PY07061	Uncharacterized protein	n/a	8	3
PY07489	Uncharacterized protein	n/a	8	3
PY01359	Uncharacterized protein	Predicted: protein binding	8	3
PY03793	Uncharacterized protein	catalytic activity	8	3
PY03273	Uncharacterized protein	n/a	8	2
PY03161	Uncharacterized protein	n/a	8	2
PY01954	Uncharacterized protein	n/a	8	2
PY00706	Uncharacterized protein	n/a	8	2
PY00521	Uncharacterized protein	n/a	8	2
PY04031	Uncharacterized protein	n/a	8	2
PY01943	Uncharacterized protein	Predicted: transferase activity	8	2
PY04619	Uncharacterized protein	n/a	8	2
PY02081	Uncharacterized protein	n/a	8	2
PY00261	Uncharacterized protein	n/a	8	2
PY00328	Putative yir1 protein	integral component of membrane	8	2
PY04664	Putative Ribosomal protein L28	structural constituent of ribosome	8	2

Peptide Hits (95%) defines the number of peptides matched to a particular protein with ≥95% confidence.
[a] Not previously reported in exosomes.

ber of vesicles for analysis. Despite this, obtaining exosomes from in vivo models is challenging, especially in comparison to obtaining exosomes from culture media. Adding to this is the fact that distinct secretomes may be presented by parasites in vivo versus in culture (Pelle et al., 2015; Brown and Guler, 2020).

Consistent with reports in the literature, results obtained herein by TEM showed that most vesicles in the microscopic field had a collapsed centre/"cup-shape". However, this commonly reported exosome morphology under TEM could be an artefact of the technique. It has been shown that vesicles can collapse during the drying process of preparation of the samples for TEM and that the resulting shape is then erroneously reported as a typical exosome feature, when in fact the vesicles are round (Conde-Vancells et al., 2008; Raposo and Stoorvogel, 2013). The size of the sEVs isolated from the plasma of *P. yoelii* 1XNL-infected mice was shown by TEM to be under 150 nm in size; this is consistent with that frequently reported in the literature (reviewed in Mathieu et al., 2019), although vesicles of about 200 nm have been identified (Duijvesz et al., 2013; Katsuda et al., 2013; Li et al., 2014). Herein, the identification of the isolated vesicles was corroborated by flow cytometry and SDS-PAGE, as reported by others (Clayton et al., 2003; Mantel et al., 2013; Keerthikumar et al., 2016), and the complementary DLS analysis confirmed the average size (median diameter of 142.2 ± 11 nm) of the exosomes. DLS analysis also showed that the exosomes isolated had a negative charge, varying between −7.36 and −0.86 mV, consistent with their ability to be distributed through the systemic circulation (Malhotra et al., 2016; Luan et al., 2017).

The assessment of total protein concentration using the Bradford protein assay indicated that mice infected with *P. yoelii* had a 2.7-fold increase in the levels of circulating sEVs at 9 days p.i., when compared with uninfected mice, and a corresponding 5.4-fold increase in total protein concentration. This result is consistent with reports from others (Nantakomol et al., 2011; Mantel et al., 2013), including a study which showed a 10-fold increase in vesicle secretion from erythrocytes for three different species of *Plasmodium* (Nantakomol et al., 2011). Our observation of incremental changes in protein content on each consecutive experimental time point might be suggestive of efficient protein trafficking into exosomes during infection. It is likely that these changes occur dynamically in response to the immune processes in the host and its bloodstream, given the processes shown to exist for active sorting of molecules into exosomes (Buschow et al., 2009; Raposo and Stoorvogel, 2013). However, it is also a possibility that the increase in total levels of vesicles at day 9 p.i. might be a consequence of the active reticulocytosis at this time of infection, or due to an increase in the release of vesicles by infected and/or uninfected cells (e.g., immune cells) in response to high parasitaemia.

In total, 489 proteins were identified in isolated and purified sEVs following in vivo infection of mice with *P. yoelii*, 17XNL pRBCs. This number is higher than that found by Martin-Jaular et al. (2011), also using a *P. yoelii* model to obtain exosomes from plasma of infected mice. The identity of the antigens described herein also somewhat differ from those described in the Martin-Jaular et al. study. These differences can be explained by the rodent malaria model used, the p.i. time point analysed (approximately 14 days p.i.), and our use of the Optiprep™ density gradient medium to isolate sEVs, increasing the purity of our preparation. It is likely that these factors have an influence on the type, number and ratio of proteins obtained in the analysis, explaining the discrepancy between these two works. Similarly, the differences between the work described herein and that described by Martin-Jaular et al. in 2016 (Martin-Jaular et al., 2016) might be a reflection of the latter using exosomes purified from the supernatant of reticulocyte cultures, rather than from an in vivo infection.

Interestingly, approximately 70% of the 489 proteins were associated with a single time point, 8 days p.i., although total protein concentration reached a maximum at 9 days p.i. This suggests that protein concentration and protein variety are not directly associated. It is possible that the uncharacterized proteins found at 8 days p.i. could include some virulence factors, since results showed that parasitaemia rose exponentially between 8 and 9 days p.i. This is consistent with a role for *Plasmodium*-derived exosomes as key regulators of the host/parasite dynamics. The proteins identified via proteomic analysis also confirmed the exosomal nature of the isolated vesicles and associated the identified sEV proteins with a number of different molecular functions, as reported by others (Raposo et al., 1996; Valadi et al., 2007; Putz et al., 2008; Camussi et al., 2011; Ludwig and Giebel, 2012; Sabin and Winn, 2012; Bartneva et al., 2013; Meckes and Goodrum, 2015). CD107a (Lamp1) was found among the contents of the sEVs purified from the plasma of infected mice, indicating that these vesicles originated from an internal compartment and were not plasma membrane fragments. The concomitant presence of Lamp1 and absence of CD40l (a microvesicle marker) and CD133 (membrane particle marker) very strongly indicate the exosomal nature of our sEV preparation, as suggested by others (Martin-Jaular et al., 2011). Also of note was the presence of macrophage-inducing factors and metalloproteases in the exosome preparations. In malaria, as well as in many other infectious diseases caused by protozoans, overexpression of metalloproteases together with increased expression of TNF-α, IFN-γ and other pro-inflammatory cytokines are conducive to parasite dispersion and increased pathogenesis (Prato et al., 2005; Bruschi and Pinto, 2013).

From a total of 489 exosomal proteins isolated from the in vivo infection with *P. yoelii*, 360 were found to be associated with the host, and 129 were associated with the parasite. A large proportion of host and parasite-derived proteins found in exosomes were associated with the immune system, biological regulation, response to stimulus and cell communication, among others. These results are consistent with reports from other groups, implicating exosomes with a large range of molecular functions and processes (Raposo et al., 1996; Valadi et al., 2007; Putz et al., 2008; Bartneva et al., 2013; Camussi et al., 2011; Ludwig and Giebel, 2012; Sabin and Winn, 2012; Mantel et al., 2013; Meckes and Goodrum, 2015).

Among the 129 parasite-associated proteins, 40 were assigned with high confidence (score $\geq$ 95%). Importantly, 23 of those have not been previously characterised and may represent novel vaccine targets. Moreover, 7/17 previously annotated proteins have not been, to the best of our knowledge, previously reported in sEVs isolated from a bloodstream infection with *P. yoelii*. Moreover, 27 of the 40 proteins, although previously reported, are yet to be characterised. Notably, among the identified proteins were the Dynein beta chain, the Asparagine-rich protein, the p235 rhoptry protein, a few proteins of the Yir family, and a ribosomal protein bearing little homology with its human homologue. These represent targets for protective immunity (i.e., vaccine targets) because they are specific to the parasite (low or no homology with the human proteins). Of note, the UBA2-related protein, which is a SUMO-activating enzyme, was the parasite protein with highest number of peptides identified in this analysis. This was an interesting result given the key role of sumoylation in the selective sorting of miRNA into exosomes (Villarroya-Beltri et al., 2013), and the growing importance of microRNA molecules in malaria (Mantel et al., 2016; Wang et al., 2017). Furthermore, this result is also consistent with the dynamics of protein expression found in the samples studied herein.

We showed that the proportion of *Plasmodium*-specific antigens contained in host sEVs, varied throughout the different infection timepoints. The dynamics of protein expression in the *P. yoelii* model suggested that protein trafficking into vesicles is an efficient process, given the changes in protein content on each consecutive experimental timepoint (7, 8 and 9 days p.i.). Together with the finding of a higher share of proteins in infected samples when compared with control mice, this is consistent with an increase in protein trafficking into sEVs during infection. This increased protein trafficking may culminate in the inclusion of parasite proteins or immunomodulatory agents into exosomes that are released from infected cells. These exosomes, containing parasite proteins, could then be internalised by macrophages and induce strong pro-inflammatory responses, initiating a loop of cytokine production/exosome release, resulting in a cascade of altered haematological and immune responses. Since these sEVs can circulate in the periphery while maintaining their integrity (consequently protecting their contents from protease degradations, for instance), and have proven capacity to activate $CD4^+$ and $CD8^+$ T cells, they represent attractive vaccine targets and potential sources of immunomodulatory agents.

Overall, herein, we identified and characterised proteins within naturally occurring sEVs of apparent exosomal nature isolated following in vivo infection with *P. yoelii* 17XNL. From a total of 489 vesicular proteins isolated from the in vivo infection with *P. yoelii*, 40 were found to be associated with the parasite, with high confidence. Importantly, 23 of those proteins have not been previously characterised and may represent novel vaccine targets. Of the 17 proteins that have been previously annotated, seven have not been previously reported in *Plasmodium* exosomes. These 17 proteins were associated with metabolic processes, homeostasis and immunity, among other functions. The apparent fast, dynamic change in protein content along the course of infection likely changes in the host bloodstream with immune status. Our data are consistent with a role for *Plasmodium*-derived exosomes in conveying stimuli or inhibitors that can influence the host systemic immune response, as well as a potential source of immune biomarkers or vaccine candidates. The results presented here contribute to the knowledge on *Plasmodium*-derived small extracellular vesicles by presenting novel information about the contents and putative roles for EVs in vivo, in a field where most studies are associated with parasites that have been derived from in vitro cultures.

Acknowledgements

This work was supported by the National Health and Medical Research Council of Australia (NHMRC Program Grant #1037304.) DLD was supported by a NHMRC Principal Research Fellowship (#1023636). KdS was supported by the University of Queensland International Postgraduate Research Scholarship, Australia.

Appendix A. Supplementary data

Supplementary data to this article can be found online at https://doi.org/10.1016/j.ijpara.2021.06.001.

References

Andreu, Z., Yanez-Mo, M., 2014. Tetraspanins in extracellular vesicle formation and function. Front. Immunol. 5, 442.

Apte, S.H., Groves, P.L., Roddick, J.S., P. da Hora, V., Doolan, D.L., 2011. High-throughput multi-parameter flow-cytometric analysis from micro-quantities of *Plasmodium*-infected blood. Int. J. Parasitol. 41 (12), 1285–1294.

Babatunde, K.A., Mbagwu, S., Hernandez-Castaneda, M.A., Adapa, S.R., Walch, M., Filgueira, L., Falquet, L., Jiang, R.H.Y., Ghiran, I., Mantel, P.Y., 2018. Malaria infected red blood cells release small regulatory RNAs through extracellular vesicles. Sci. Rep. 8, 884.

Bartneva, N.S., Maltsev, N., Vorobjev, I.A., 2013. Microvesicles and intercellular communication in the context of parasitism. Front. Cell. Infect. Microbiol. 3, 49.

Bayer-Santos, E., Aguilar-Bonavides, C., Rodrigues, S.P., Cordero, E.M., Marques, A.F., Varela-Ramirez, A., Choi, H., Yoshida, N., da Silveira, J.F., Almeida, I.C., 2013. Proteomic analysis of *Trypanosoma cruzi* secretome: characterization of two populations of extracellular vesicles and soluble proteins. J. Proteome Res. 12 (2), 883–897.

Bhatnagar, S., Shinagawa, K., Castellino, F.J., Schorey, J.S., 2007. Exosomes released from macrophages infected with intracellular pathogens stimulate a proinflammatory response *in vitro* and *in vivo*. Blood 110, 3234–3244.

Brown, A.C., Guler, J.L., 2020. From circulation to cultivation: *Plasmodium in vivo* versus *in vitro*. Trends Parasitol. 36 (11), 914–926.

Bruschi, F., Pinto, B., 2013. The significance of matrix metalloproteinases in parasitic infections involving the Central Nervous System. Pathogens 2 (1), 105–129.

Buschow, S.I., Nolte-'t Hoen, E.N., van Niel, G., Pols, M.S., ten Broeke, T., Lauwen, M., Ossendorp, F., Melief, C.J., Raposo, G., Wubbolts, R., Wauben, M.H., Stoorvogel, W., 2009. MHC II in dendritic cells is targeted to lysosomes or T cell-induced exosomes via distinct multivesicular body pathways. Traffic 10, 1528–1542.

Camussi, G., Deregibus, M.C., Bruno, S., Grange, C., Fonsato, V., Tetta, C., 2011. Exosome/microvesicle-mediated epigenetic reprogramming of cells. Am. J. Cancer Res. 1, 98–110.

Chaput, N., Théry, C., 2011. Exosomes: immune properties and potential clinical implementations. Sem. Immunopathol. 33 (5), 419–440.

Clark, I.A., Rockett, K.A., 1994. The cytokine theory of human cerebral malaria. Parasitol. Today 10 (10), 410–412.

Clayton, A., Harris, C., Court, J., Mason, M.D., Morgan, B.P., 2003. Antigen-presenting cell exosomes are protected from complement-mediated lysis by expression of CD55 and CD59. Eur. J. Immunol. 33 (2), 522–531.

Combes, V., Taylor, T.E., Juhan Vague, I., Mege, J.L., Mwenechanya, J., Tembo, M., Grau, G.E., Molyneux, M.E., 2004. Circulating endothelial microparticles in Malawian children with severe falciparum malaria complicated with coma. JAMA 291.

Conde-Vancells, J., Rodriguez-Suarez, E., Embade, N., Gil, D., Matthiesen, R., Valle, M., Elortza, F., Lu, S.C., Mato, J.M., Falcon-Perez, J.M., 2008. Characterization and comprehensive proteome profiling of exosomes secreted by hepatocytes. J. Proteome Res. 7 (12), 5157–5166.

Couper, K.N., Barnes, T., Hafalla, J.C.R., Combes, V., Ryffel, B., Secher, T., Grau, G.E., Riley, E.M., de Souza, J.B., Kazura, J.W., 2010. Parasite-derived plasma microparticles contribute significantly to malaria infection-induced inflammation through potent macrophage stimulation. PLoS Pathog. 6 (1), 1000744.

Demarta-Gatsi, C., Rivkin, A., Di Bartolo, V., Peronet, R., Ding, S., Commere, P.-H., Guillonneau, F., Bellalou, J., Brûlé, S., Abou Karam, P., Cohen, S.R., Lagache, T., Janse, C.J., Regev-Rudzki, N., Mécheri, S., 2019. Histamine releasing factor and elongation factor 1 alpha secreted via malaria parasites extracellular vesicles promote immune evasion by inhibiting specific T cell responses. Cell. Microbiol. 21 (7), e13021.

Deolindo, P., Evans-Osses, I., Ramirez, M.I., 2013. Microvesicles and exosomes as vehicles between protozoan and host cell communication. Biochem. Soc. Trans. 41, 252–257.

Dinglasan, R.R., Armistead, J.S., Nyland, J.F., Jiang, X., Mao, H.Q., 2013. Single-dose microparticle delivery of a malaria transmission-blocking vaccine elicits a long-lasting functional antibody response. Curr. Mol. Med. 13, 479–487.

Drurey, C., Coakley, G., Maizels, R.M., 2020. Extracellular vesicles: new targets for vaccines against helminth parasites. Int. J. Parasitol. 50 (9), 623–633.

Duijvesz, D., Burnum-Johnson, K.E., Gritsenko, M.A., Hoogland, A.M., Vredenbregt-van den Berg, M.S., Willemsen, R., Luider, T., Paša-Tolić, L., Jenster, G., Culig, Z., 2013. Proteomic profiling of exosomes leads to the identification of novel biomarkers for prostate cancer. PLoS ONE 8 (12), e82589.

Fevrier, B., Vilette, D., Archer, F., Loew, D., Faigle, W., Vidal, M., Laude, H., Raposo, G., 2004. Cells release prions in association with exosomes. Proc. Natl. Acad .Sci. U S A 101 (26), 9683–9688.

Geiger, A., Hirtz, C., Bécue, T., Bellard, E., Centeno, D., Gargani, D., Rossignol, M., Cuny, G., Peltier, J.B., 2010. Exocytosis and protein secretion in *Trypanosoma*. BMC Microbiol. 10 (1), 20. https://doi.org/10.1186/1471-2180-10-20.

Giri, P.K., Schorey, J.S., Bishai, W., 2008. Exosomes derived from M. Bovis BCG infected macrophages activate antigen-specific $CD4^+$ and $CD8^+$ T cells in vitro and in vivo. PLoS ONE 3 (6), e2461.

Gould, S.J., Booth, A.M., Hildreth, J.E.K., 2003. The Trojan exosome hypothesis. Proc. Natl. Acad. Sci. U S A 100 (19), 10592–10597.

Gutzeit, C., Nagy, N., Gentile, M., Lyberg, K., Gumz, J., Vallhov, H., Puga, I., Klein, E., Gabrielsson, S., Cerutti, A., Scheynius, A., 2014. Exosomes derived from Burkitt's lymphoma cell lines induce proliferation, differentiation, and class-switch recombination in B cells. J. Immunol. 192 (12), 5852–5862.

Hosseini-Beheshti, E., Pham, S., Adomat, H., Li, N.a., Tomlinson Guns, E.S., 2012. Exosomes as biomarker enriched microvesicles: characterization of exosomal proteins derived from a panel of prostate cell lines with distinct AR phenotypes. Mol. Cell Prot. 11 (10), 863–885.

Hwang, I., 2013. Cell-cell communication via extracellular membrane vesicles and its role in the immune response. Mol. Cells 36 (2), 105–111.

Instruments, 2009. ZetaSizer User Manual. Worcestershire, United Kingdom.

Jeppesen, D.K., Fenix, A.M., Franklin, J.L., Higginbotham, J.N., Zhang, Q., Zimmerman, L.J., Liebler, D.C., Ping, J., Liu, Q., Evans, R., Fissell, W.H., Patton, J.G., Rome, L.H., Burnette, D.T., Coffey, R.J., 2019. Reassessment of exosome composition. Cell 177 (2), 428–445.e18.

Katsuda, T., Tsuchiya, R., Kosaka, N., Yoshioka, Y., Takagaki, K., Oki, K., Takeshita, F., Sakai, Y., Kuroda, M., Ochiya, T., 2013. Human adipose tissue-derived mesenchymal stem cells secrete functional neprilysin-bound exosomes. Sci. Rep. 3, 1197.

Keerthikumar, S., Chisanga, D., Ariyaratne, D., Al Saffar, H., Anand, S., Zhao, K., Samuel, M., Pathan, M., Jois, M., Chilamkurti, N., Gangoda, L., Mathivanan, S., 2016. ExoCarta: A web-based compendium of exosomal cargo. J. Mol. Biol. 428 (4), 688–692.

Kowal, J., Arras, G., Colombo, M., Jouve, M., Morath, J.P., Primdal-Bengtson, B., Dingli, F., Loew, D., Tkach, M., Théry, C., 2016. Proteomic comparison defines novel markers to characterize heterogeneous populations of extracellular vesicle subtypes. Proc. Natl. Acad. Sci. U S A 113 (8), E968–E977.

Li, M., Zeringer, E., Barta, T., Schageman, J., Cheng, A., Vlassov, A.V., 2014. Analysis of the RNA content of the exosomes derived from blood serum and urine and its potential as biomarkers. Philos. Trans. Roy. Soc. Biol. 369 (1652), 20130502.

Lötvall, J., Hill, A.F., Hochberg, F., Buzás, E.I., Di Vizio, D., Gardiner, C., Gho, Y.S., Kurochkin, I.V., Mathivanan, S., Quesenberry, P., Sahoo, S., Tahara, H., Wauben, M.H., Witwer, K.W., Théry, C., 2014. Minimal experimental requirements for definition of extracellular vesicles and their functions: a position statement from the International Society for Extracellular Vesicles. J. Extracell Ves. 3 (1), 26913.

Luan, X., Sansanaphongpricha, K., Myers, I., Chen, H., Yuan, H., Sun, D., 2017. Engineering exosomes as refined biological nanoplatforms for drug delivery. Acta Pharmacol. Sin. 38 (6), 754–763.

Ludwig, A.-K., Giebel, B., 2012. Exosomes: small vesicles participating in intercellular communication. Int. J. Biochem. Cell Biol. 44 (1), 11–15.

Malhotra, H., Sheokand, N., Kumar, S., Chauhan, A.S., Kumar, M., Jakhar, P., Boradia, V.M., Raje, C.I., Raje, M., 2016. Exosomes: tunable nano vehicles for macromolecular delivery of transferrin and lactoferrin to specific intracellular compartment. J. Biomed. Nanotechnol. 12 (5), 1101–1114.

Mantel, P.Y., Hjelmqvist, D., Walch, M., Kharoubi-Hess, S., Nilsson, S., Ravel, D., Ribeiro, M., Gruring, C., Ma, S., Padmanabhan, P., Trachtenberg, A., Ankarklev, J., Brancucci, N.M., Huttenhower, C., Duraisingh, M.T., Ghiran, I., Kuo, W.P., Filgueira, L., Martinelli, R., Marti, M., 2016. Infected erythrocyte-derived extracellular vesicles alter vascular function via regulatory Ago2-miRNA complexes in malaria. Nat. Commun. 7, 12727.

Mantel, P.-Y., Hoang, A.N., Goldowitz, I., Potashnikova, D., Hamza, B., Vorobjev, I., Ghiran, I., Toner, M., Irimia, D., Ivanov, A.R., Barteneva, N., Marti, M., 2013. Malaria-infected erythrocyte-derived microvesicles mediate cellular communication within the parasite population and with the host immune system. Cell Host Microbe 13 (5), 521–534.

Mantel, P.-Y., Marti, M., 2014. The role of extracellular vesicles in *Plasmodium* and other protozoan parasites. Cell. Microbiol. 16 (3), 344–354.

Martin-Jaular, L., de Menezes-Neto, A., Monguio-Tortajada, M., Elizalde-Torrent, A., Diaz-Varela, M., Fernandez-Becerra, C., Borras, F.E., Montoya, M., Del Portillo, H. A., 2016. Spleen-Dependent Immune Protection Elicited by CpG Adjuvanted reticulocyte-derived exosomes from malaria infection is associated with changes in T cell subsets' distribution. Front. Cell Develop. Biol. 4, 131.

Martín-Jaular, L., de Menezes-Neto, A., Monguió-Tortajada, M., Elizalde-Torrent, A., Díaz-Varela, M., Fernández-Becerra, C., Borras, F.E., Montoya, M., del Portillo, H. A., 2016. Spleen-dependent immune protection elicited by CpG adjuvanted reticulocyte-derived exosomes from malaria infection is associated with changes in T cell subsets' distribution. Front. Cell Develop. Biol. 4, 131.

Martin-Jaular, L., Nakayasu, E.S., Ferrer, M., Almeida, I.C., del Portillo, H.A., Rénia, L., 2011. Exosomes from *Plasmodium yoelii*-Infected reticulocytes protect mice from lethal infections. PLoS ONE 6 (10), e26588.

Mathieu, M., Martin-Jaular, L., Lavieu, G., Théry, C., 2019. Specificities of secretion and uptake of exosomes and other extracellular vesicles for cell-to-cell communication. Nat. Cell Biol. 21 (1), 9–17.

Meckes, D.G., Goodrum, F., 2015. Exosomal communication goes viral. J. Virol. 89 (10), 5200–5203.

Mekonnen, G.G., Pearson, M., Loukas, A., Sotillo, J., 2018. Extracellular vesicles from parasitic helminths and their potential utility as vaccines. Expert Rev. Vacc. 17 (3), 197–205.

Mi, H., Muruganujan, A., Casagrande, J.T., Thomas, P.D., 2013. Large-scale gene function analysis with the PANTHER classification system. Nat. Prot. 8 (8), 1551–1566.

Mittelbrunn, M., Sánchez-Madrid, F., 2012. Intercellular communication: diverse structures for exchange of genetic information. Nat. Rev. Mol. Cell Biol. 13 (5), 328–335.
Montaner-Tarbes, S., Borras, F.E., Montoya, M., Fraile, L., Del Portillo, H.A., 2016. Serum-derived exosomes from non-viremic animals previously exposed to the porcine respiratory and reproductive virus contain antigenic viral proteins. Vet. Res. 47, 59.
Montecalvo, A., Shufesky, W.J., Beer Stolz, D., Sullivan, M.G., Wang, Z., Divito, S.J., Papworth, G.D., Watkins, S.C., Robbins, P.D., Larregina, A.T., Morelli, A.E., 2008. Exosomes as a short-range mechanism to spread alloantigen between dendritic cells during T cell allorecognition. J. Immunol. 180 (5), 3081–3090.
Nantakomol, D., Dondorp, A.M., Krudsood, S., Udomsangpetch, R., Pattanapanyasat, K., Combes, V., Grau, G.E., White, N.J., Viriyavejakul, P., Day, N.P., Chotivanich, K., 2011. Circulating red cell-derived microparticles in human malaria. J. Infect. Dis. 203, 700–706.
Nguyen, D.G., Booth, A., Gould, S.J., Hildreth, J.E.K., 2003. Evidence that HIV budding in primary macrophages occurs through the exosome release pathway. J. Biol. Chem. 278 (52), 52347–52354.
Padro, C.J., Shawler, T.M., Gormley, M.G., Sanders, V.M., 2013. Adrenergic regulation of IgE Involves modulation of CD23 and ADAM10 expression on exosomes. J. Immunol. 191 (11), 5383–5397.
Pelle, K.G., Oh, K., Buchholz, K., Narasimhan, V., Joice, R., Milner, D.A., Brancucci, N., Ma, S., Voss, T.S., Ketman, K., Seydel, K.B., Taylor, T.E., Barteneva, N.S., Huttenhower, C., Marti, M., 2015. Transcriptional profiling defines dynamics of parasite tissue sequestration during malaria infection. Genome Med. 7 (1), 19. https://doi.org/10.1186/s13073-015-0133-7.
Peterson, M.F., Otoc, N., Sethi, J.K., Gupta, A., Antes, T.J., 2015. Integrated systems for exosome investigation. Methods 87, 31–45.
Prato, M., Giribaldi, G., Polimeni, M., Gallo, V., Arese, P., 2005. Phagocytosis of hemozoin enhances matrix metalloproteinase-9 activity and tnf-α production in human monocytes: role of matrix metalloproteinases in the pathogenesis of falciparum malaria. J. Immunol. 175 (10), 6436–6442.
Putz, U., Howitt, J., Lackovic, J., Foot, N., Kumar, S., Silke, J., Tan, S.-S., 2008. Nedd4 family-interacting protein 1 (Ndfip1) is required for the exosomal secretion of Nedd4 family proteins. J. Biol. Chem. 283 (47), 32621–32627.
Raposo, G., Nijman, H.W., Stoorvogel, W., Leijendekker, R., Harding, C.V., Melief, C.J. M., Geuze, H.J., 1996. B lymphocytes secrete antigen-presenting vesicles. J. Exp. Med. 183, 1161–1172.
Raposo, G., Stoorvogel, W., 2013. Extracellular vesicles: Exosomes, microvesicles, and friends. J. Cell Biol. 200, 373–383.
Rechavi, O., Goldstein, I., Kloog, Y., 2009. Intercellular exchange of proteins: the immune cell habit of sharing. FEBS Lett. 583, 1792–1799.
Regev-Rudzki, N., Wilson, D.W., Carvalho, T.G., Sisquella, X., Coleman, B.M., Rug, M., Bursac, D., Angrisano, F., Gee, M., Hill, A.F., Baum, J., Cowman, A.F., 2013. Cell-cell communication between malaria-infected red blood cells via exosome-like vesicles. Cell 153 (5), 1120–1133.
Robbins, P.D., Morelli, A.E., 2014. Regulation of immune responses by extracellular vesicles. Nat. Rev. Immunol. 14 (3), 195–208.
Sabin, K.Z., Winn, R.J., 2012. Abstract 5406: Glioblastoma derived exosomes induce apoptosis in T cells. Cancer Res. 72, 5406–5406.
Sampaio, N.G., Cheng, L., Eriksson, E.M., 2017. The role of extracellular vesicles in malaria biology and pathogenesis. Malar. J. 16, 245.
Sampaio, N.G., Emery, S.J., Garnham, A.L., Tan, Q.Y., Sisquella, X., Pimentel, M.A., Jex, A.R., Regev-Rudzki, N., Schofield, L., Eriksson, E.M., 2018. Extracellular vesicles from early stage *Plasmodium falciparum*-infected red blood cells contain PfEMP1 and induce transcriptional changes in human monocytes. Cell. Microbiol. 20 (5), e12822.
Schorey, J.S., Cheng, Y., Singh, P.P., Smith, V.L., 2015. Exosomes and other extracellular vesicles in host–pathogen interactions. EMBO Rep. 16 (1), 24–43.
Shenoda, B.B., Ajit, S.K., 2016. Modulation of immune responses by exosomes derived from antigen-presenting cells. Clin. Med. Insights Pathol. 9, 1–8.
Silverman, J.M., Reiner, N.E., 2012. *Leishmania* exosomes deliver preemptive strikes to create an environment permissive for early infection. Front. Cell. Infect. Microbiol. 1, 26.
Sisquella, X., Ofir-Birin, Y., Pimentel, M.A., Cheng, L., Abou Karam, P., Sampaio, N.G., Penington, J.S., Connolly, D., Giladi, T., Scicluna, B.J., Sharples, R.A., Waltmann, A., Avni, D., Schwartz, E., Schofield, L., Porat, Z., Hansen, D.S., Papenfuss, A.T., Eriksson, E.M., Gerlic, M., Hill, A.F., Bowie, A.G., Regev-Rudzki, N., 2017. Malaria parasite DNA-harbouring vesicles activate cytosolic immune sensors. Nat. Commun. 8, 1985.
Thery, C., Duban, L., Segura, E., Veron, P., Lantz, O., Amigorena, S., 2002. Indirect activation of naive $CD4^+$ T cells by dendritic cell-derived exosomes. Nat. Immunol. 3, 1156–1162.
Théry, C., Witwer, K.W., Aikawa, E., Alcaraz, M.J., Anderson, J.D., Andriantsitohaina, R., Antoniou, A., Arab, T., Archer, F., Atkin-Smith, G.K.J.J.o.e.v., 2018. Minimal information for studies of extracellular vesicles 2018 (MISEV2018): a position statement of the International Society for Extracellular Vesicles and update of the MISEV2014 guidelines. J. Extracell Ves. 7, 1.
Toda, H., Diaz-Varela, M., Segui-Barber, J., Roobsoong, W., Baro, B., Garcia-Silva, S., Galiano, A., Gualdron-Lopez, M., Almeida, A.C.G., Brito, M.A.M., de Melo, G.C., Aparici-Herraiz, I., Castro-Cavadia, C., Monteiro, W.M., Borras, E., Sabido, E., Almeida, I.C., Chojnacki, J., Martinez-Picado, J., Calvo, M., Armengol, P., Carmona-Fonseca, J., Yasnot, M.F., Lauzurica, R., Marcilla, A., Peinado, H., Galinski, M.R., Lacerda, M.V.G., Sattabongkot, J., Fernandez-Becerra, C., Del Portillo, H.A., 2020. Plasma-derived extracellular vesicles from *Plasmodium vivax* patients signal spleen fibroblasts via NF-kB facilitating parasite cytoadherence. Nat. Commun. 11, 2761.
Valadi, H., Ekström, K., Bossios, A., Sjöstrand, M., Lee, J.J., Lötvall, J.O., 2007. Exosome-mediated transfer of mRNAs and microRNAs is a novel mechanism of genetic exchange between cells. Nat. Cell Biol. 9 (6), 654–659.
Villarroya-Beltri, C., Gutiérrez-Vázquez, C., Sánchez-Cabo, F., Pérez-Hernández, D., Vázquez, J., Martin-Cofreces, N., Martinez-Herrera, D.J., Pascual-Montano, A., Mittelbrunn, M., Sánchez-Madrid, F., 2013. Sumoylated hnRNPA2B1 controls the sorting of miRNAs into exosomes through binding to specific motifs. Nat. Commun. 4, 2980.
Vlassov, A.V., Magdaleno, S., Setterquist, R., Conrad, R., 2012. Exosomes: current knowledge of their composition, biological functions, and diagnostic and therapeutic potentials. Biochim. Biophys. Acta, Mol. Cell. Biol. Lipids 1820 (7), 940–948.
Wang, Z., Xi, J., Hao, X., Deng, W., Liu, J., Wei, C., Gao, Y., Zhang, L., Wang, H., 2017. Red blood cells release microparticles containing human argonaute 2 and miRNAs to target genes of *Plasmodium falciparum*. Emerg. Microbiol. Infect. 6 (1), 1–11.
Willms, E., Cabanas, C., Mager, I., Wood, M.J.A., Vader, P., 2018. Extracellular vesicle heterogeneity: subpopulations, isolation techniques, and diverse functions in cancer progression. Front. Immunol. 9, 738.
Wiśniewski, J.R., Zougman, A., Nagaraj, N., Mann, M., 2009. Universal sample preparation method for proteome analysis. Nat. Methods 6 (5), 359–362.
Yanez-Mo, M., Siljander, P.R., Andreu, Z., Zavec, A.B., Borras, F.E., Buzas, E.I., Buzas, K., Casal, E., Cappello, F., Carvalho, J., Colas, E., Cordeiro-da Silva, A., Fais, S., Falcon-Perez, J.M., Ghobrial, I.M., Giebel, B., Gimona, M., Graner, M., Gursel, I., Gursel, M., Heegaard, N.H., Hendrix, A., Kierulf, P., Kokubun, K., Kosanovic, M., Kralj-Iglic, V., Kramer-Albers, E.M., Laitinen, S., Lasser, C., Lener, T., Ligeti, E., Line, A., Lipps, G., Llorente, A., Lotvall, J., Mancek-Keber, M., Marcilla, A., Mittelbrunn, M., Nazarenko, I., Nolte-'t Hoen, E.N., Nyman, T.A., O'Driscoll, L., Olivan, M., Oliveira, C., Pallinger, E., Del Portillo, H.A., Reventos, J., Rigau, M., Rohde, E., Sammar, M., Sanchez-Madrid, F., Santarem, N., Schallmoser, K., Ostenfeld, M.S., Stoorvogel, W., Stukelj, R., Van der Grein, S.G., Vasconcelos, M. H., Wauben, M.H., De Wever, O., 2015. Biological properties of extracellular vesicles and their physiological functions. J Extracell Ves 4, 27066.